

dendritic branch for a duration of 0.5 ms with a linear shift in the onset with respect to distance. The somatic onset of depolarization was defined as zero time and 0.5 ms at the uppermost branches. The overall membrane potential waveform at somatic level is shown in Fig. 6 B and was considered an adequate analog of the experimental data. Thus, the large initial spike is followed by a second depolarization of about 50–60% amplitude and a set of such wavelets which wax and wane.

Display of membrane potential change along the cell puts in evidence a possible mechanism for the generation of the waveform. Apparently the peaks of the burst are generated by the repetitive firing of the initial segment (followed shortly by the somatic firing) rather than in the dendrites as originally proposed (ECCLES *et al.*, 1966; MARTINEZ *et al.*, 1971). It is clear that in this model the firing pattern is evoked by the delayed repolarization of the dendritic tree which drives the somatic and initial segment compartments into a short burst of repetitive firing. The model also suggests a possible explanation for the fragile nature of some of the spike peaks, as opposed to the stable components of this burst. Furthermore, the results are consistent with similar findings in the cat Purkinje cells. For instance, the last of the three spike wavelets in the climbing fiber bursts shows the most variability (also in extracellular records) (cf. LLINÁS & VOLKIND, 1973). As indicated by the model, this phenomenon may be produced by the antidromic invasion of the propagating axonal action potential into the soma. This feature appears to result from the impedance mismatch and loose coupling of the somatic and the initial segment and axon regions, due to morphological and excitability differences.

Similar phenomenology may also be found using a different dendritic branch configuration with parameters otherwise identical to those of the model used

in Fig. 6. One such example is illustrated in Fig. 7 A and B, where the basic pattern of complex spike is similar to the previous case. This is in accordance with the fact that the complex spike waveform is a highly stereotyped response, quite similar from cell to cell, although these cells exhibit more than trivial morphological differences.

Reversal of the climbing fiber evoked EPSP

The reversal properties of EPSP evoked by a climbing fiber-like activation is illustrated in Fig. 8 B. Figure 8 A shows actual intracellular recordings from a cat Purkinje cell, the EPSP showing a characteristic biphasic reversal as a depolarizing current of increasing amplitude is applied across the somatic membrane (LLINÁS & NICHOLSON, 1976). As seen in Fig. 8 B in a purely passive model with an E_{EPSP} of -10 mV, the results from the model show striking similarities with the experimental results, even in quantitative terms. The biphasic reversal of climbing fiber-evoked EPSP at 11.7 nA outward current injection is shown in detail in Fig. 8 C. As expected from theoretical treatment of distributed synaptic inputs (RALL, 1967; CALVIN, 1969), the EPSP in the upper branches is not reversed, producing the late depolarizing portion of the biphasic EPSP reversal.

Modification of branching and internal resistance parameters

The functional importance of different parameters in this model can also be studied with great ease. Given the large number of possible permutations of these parameters, only one representative example will be illustrated. The antidromic invasion of a Purkinje cell is shown after the introduction of two small changes in the model (Fig. 9 A), and the results may be compared to those shown in Fig. 3. In the present case the branching power is set to 1.25 and the inter-

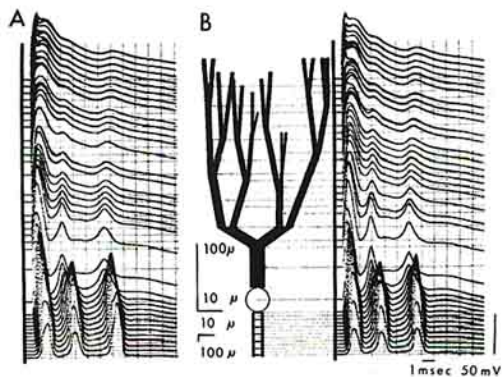


FIG. 7. Modification of climbing fiber response of Purkinje cell with slightly different excitability of soma (A) or slightly different arborization of dendritic tree (B). As shown by both numerical solutions, the general pattern of complex spike is remarkably insensitive to these changes. The only difference (as compared to Fig. 6 B) is the lack of the last wavelet.